Piezochromism in Dynamic Three-Dimensional Covalent Organic Frameworks

Jing Fang,[†][a] Zhiyuan Fu,[†][b] Xiaohong Chen,[a] Yaozu Liu,[a] Fengqian Chen,[a] Yujie Wang,[a] Hui Li,[a] Yusran Yusran,[a] Kai Wang,*[b] Valentin Valtchev,[c] Shilun Qiu,[a] Bo Zou,*[b] and Qianrong Fang*[a]

[a]   J. Fang, X. Chen, Y. Liu, F. Chen, Dr. Y. Wang, Dr. H. Li, Dr. Y. Yusran, Prof. S. Qiu and Prof. Q. Fang
       State Key Laboratory of Inorganic Synthesis and Preparative Chemistry, Department of Chemistry
       Jilin University, Changchun 130012, China
       E-mail: qrfang@jlu.edu.cn
[b]   Z. Fu, Prof. K. Wang and Prof. B. Zou
       State Key Laboratory of Superhard Materials, College of Physics
       Jilin University, Changchun 130012, P. R. China.
       E-mail: kaiwang@jlu.edu.cn or zoubo@jlu.edu.cn
[c]   Prof. V. Valtchev
       Qingdao Institute of Bioenergy and Bioprocess Technology, Chinese Academy of Sciences, 189 Songling Road, Qingdao 266101, P. R. China
       Normandie Univ, ENSICAEN, UNICAEN, CNRS, Laboratoire Catalyse et Spectrochimie, 6 Marechal Juin, 14050 Caen, France
[†]   These authors contributed equally to this work.

       Supporting information for this article is given via a link at the end of the document.

Abstract: Piezochromic materials with pressure-dependent photoluminescence-tuning properties are important in many fields, such as mechanical sensors, security papers, and storage devices. Covalent organic frameworks (COFs), as an emerging class of crystalline porous materials (CPMs), feature structural dynamics and tunable photophysical properties, which are suitable for designing piezochromic materials, but related research is scarce. Herein, we report two dynamic three-dimensional COFs based on aggregation-induced emission (AIE) or aggregation-caused quenching (ACQ) chromophores, termed JUC-635 and JUC-636, and for the first time, study their piezochromic behavior by diamond anvil cell technique. Due to the various luminescent groups, JUC-635 has completely different solvatochromism and molecular aggregation behavior in the solvents. More importantly, JUC-635 with AIE effect exhibited a maintained fluorescence with increasing pressure (~3 GPa), and a reversible sensitivity with high-contrast emission differences ($\Delta\lambda_{em}$ = 187 nm) up to 12 GPa, which is superior to other CPMs reported so far. Therefore, this research will open a new gate for expanding the potential applications of COFs as exceptional piezochromic materials in pressure sensing, barcoding, and signal switching.

Materials that change structures and emissions in response to external stimuli, such as light, heat, and pressure, are attracting increasing attention, which is considered "smart" or "dynamic" and can be functionalized as stimuli-responsive materials.[1] Owing to the dynamic of frameworks and highly tunable luminescence, crystalline porous materials (CPMs) has exhibited a variety of stimuli-response behaviors, such as photochromism,[2] solvatochromism,[3] thermochromism[4] and piezochromism,[5] which broaden their application in advanced photoelectronic, signal processing, and so on.[6] Especially piezochromic (also known as mechanochromic) materials with pressure-dependent photoluminescence-tuning properties are of great importance in such fields as mechanical sensors, security papers, storage devices, etc.[7] This highly desirable property is most often exemplified by metal−organic frameworks (MOFs), one of the typical CPMs.[8] However, except for a few materials constructed by flexible ligands, most MOFs showed a weak piezochromic behavior due to their rigid frameworks.

As an emerging class of CPMs, covalent organic frameworks (COFs),[9] constructed by linking molecular building blocks through covalent bonds, have also been demonstrated to show crystal transformation and dynamic behavior in response to light,[10] guest molecules,[11] pH,[12] and temperature.[13] Although many efforts have been made in this field,[14] little is known about piezochromism in COFs, especially the extreme pressure generated by diamond anvil cell (DAC) device that can induce dramatic changes and novel phenomena by modulating the molecular packing modes and conformation without destroying the crystalline state.[15] Currently, only a few relevant cases of COFs have been reported, including the mechanical properties by DAC[16] and the piezochromic by griding.[17] However, the former only focused on the single stimulus of pressure, and the anisotropic pressure used in the latter was often accompanied by irreversible fluorescence and the destruction of the crystalline state. What piezochromic properties can be expected for COFs by DAC have not been given yet. In principle, different from rigid MOF materails, the breathing flexibility,[18] resulting from the rotation of the imine bonds in the 3D interpenetrating networks of COFs, demonstrates the dynamic of a framework, which may show the pressure-responsive behavior by conformational transition. Meanwhile, tunable and reversible piezochromism may be induced by arranging unique chromophores as active stimuli sites, such as aggregation-induced emission luminogens (AIEgens) or aggregation-caused quenching luminogens (ACQgens), into well-defined structures of 3D COFs to control the photophysical processes. Furthermore, by rationally designing the structures, the space deformation induced by outer stimuli can act as a "secondary stimulus" to trigger and regulate the conformational changes of the organic chromophore.[19] Therefore, the dynamic mode and pressure-responsiveness of 3D COFs should be easily achieved through reasonably regulate

predesignable frameworks from engineered topology and well-defined organic chromophores. All these together make 3D COFs a potential platform for the development of highly-contrast piezochromic materials.

Taking the aforementioned considerations in mind, we herein designed two imine-linked 3D COFs, termed JUC-635 and JUC-636 (JUC = Jilin University China), featuring dynamic frameworks and unique chromophores. By rationally regulating the structures, these COFs exhibited completely different solvatochromism, in which JUC-635 consisting of AIEgens triphenylamine (TPA) group showed intramolecular charge-transfer (ICT) properties and AIE phenomenon, while JUC-636 without TPA group had an ACQ effect. Furthermore, piezochromic properties of both COFs in the solid states were explored. Compared to the continuous fluorescence reduction with increasing pressure shown by JUC-636, JUC-635 maintained its fluorescence before 3 GPa and exhibited a reversible piezofluorochromism with high-contrast emission differences ($\Delta\lambda_{em}$ = 187 nm) upon 12 GPa, which is superior to other CPMs reported so far. To the best of our knowledge, this work represents the first piezochromic COFs by DAC technique, which will open a new gate for developing COF-based piezochromic materials.

Our strategy introduces a D–A conjugated molecule (TPA-BI , Figure 1a), in which a twisted molecular motor containing three freely-rotating benzene rings (triphenylamine, TPA) can act as an electron-donating moiety linked with an electron-deficient benzimidazole (BI). Due to the unique configuration, TPA-BI was more likely to undergo configurational transitions under mechanical force in most piezochromic cases.[20] At the same time, a benzisothiadiazole derivative without rotor TPA , namely BTD, was also chosen for comparison (Figure 1b). Both TPA-BI and BTD were designed as linear building units, and tetra-(4-aminophenyl)methane (TAPM, Figure 1c) was used as a typical tetrahedral building unit. The condensation of TPA-BI or BTD with TAPM produced two novel 3D COFs, JUC-635 and JUC-636, respectively (Figure 1d,e). In light of linking such prolonged linear and tetrahedral building units, these COFs were expected to be highly interpenetrated **dia** nets (Figure 1f). It should be noted that JUC-635 with twisted rotor TPA incorporated as side chains is quite different from most AIEgen-based COFs, in which AIEgen groups (TPA) are locked on their backbone. That means we will obtain a sensitive piezochromic material without perturbing the intrinsic framework dynamics while preserving the accompanying conformational variations of the chromophore (Figure 1g).

These COFs were fabricated by the Schiff-base condensation of TPA-BI or BTD and TAPM in a mixed solvent system of mesitylene and 1,4-dioxane with acetic acid followed by heating at 120 °C for 3 days. A variety of methods were used for structural characterizations. The morphology was studied by scanning electron microscopy (SEM) and transmission electron microscopy (TEM), and both materials showed uniform fusiform-like polycrystalline morphology (Figure S1, Supporting Information). Fourier-transformed infrared (FT-IR) analysis clearly revealed the formation of new C=N stretching bands at 1609 for JUC-635 and 1611 cm^{-1} for JUC-636, respectively. The disappearance of the C=O stretching vibration (at 1690 and 1693 cm^{-1} for TPA-BI and BTD, respectively) and the N-H stretching vibration (at 3390 cm^{-1} for TAPM) confirmed the complete consumption of the building units (Figure S2). The solid-state ^{13}C cross-polarization magic-angle-spinning (CP/MAS) NMR spectroscopy further confirmed the successful synthesis of both
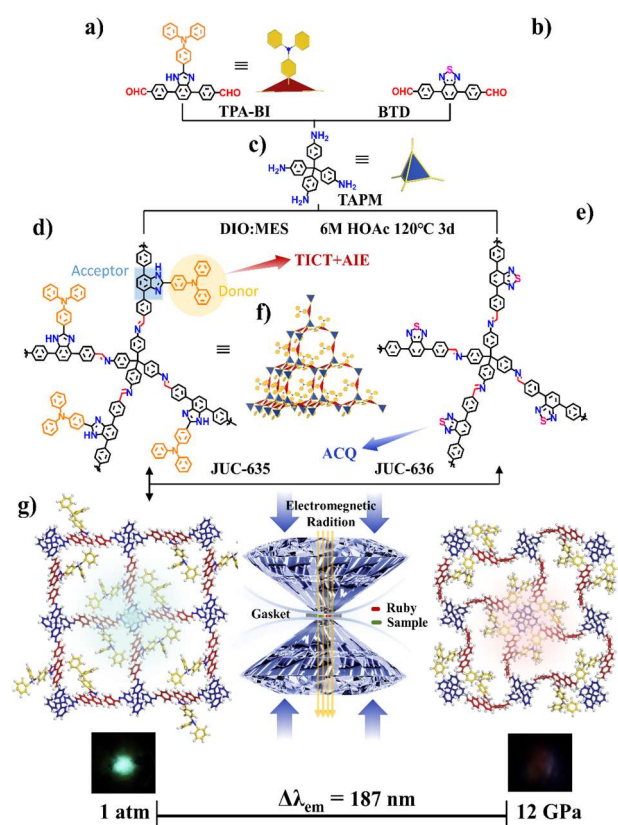

Figure 1. Condensation of linear TPA-BI (a) or BTD (b) and tetrahedral TAPM (c) to produce two dynamic 3D COFs, JUC-635 (d) and JUC-636 (e), which have 10-fold interpenetrated dia net (f). These materials were further used to study the piezochromic behavior, which showed the structural transformation under mechanical stimuli by DAC technique (g).

COFs with a characteristic resonance peak at ~158 ppm, attributable to the imine-carbon of COFs (Figure S3). Meanwhile, both COFs were stable up to about 400 °C under a nitrogen atmosphere according to the thermogravimetric analysis (TGA) (Figure S4).

The crystallinity and unit cell parameters of the COFs were verified by powder X-ray diffraction (PXRD) measurement combined with the structural simulation using the Materials Studio software package (Figure 2a,b). After geometrical energy minimization based on 10-fold interpenetrated **dia** topology, the unit cell parameters were obtained ($a = b$ = 29.35 Å, c = 7.55 Å, $\alpha = \beta = \gamma$ = 90° and $a = b$ = 28.84 Å, c = 7.31 Å, $\alpha = \beta = \gamma$ = 90° for JUC-635 and JUC-636, respectively). The simulated PXRD patterns were in good agreement with the experimental results. Full-profile pattern matching (Pawley) refinement was performed on the experimental data from solvated samples. The PXRD peaks of JUC-635 at 4.25°, 6.02°, 6.75°, 8.54° and 12.78° correspond to (110), (200), (210), (220) and (330) Bragg peaks of space group *P*-4 (No. 81), while the PXRD peaks of JUC-636 at 4.25°, 6.03°, 6.74°, 8.51° and 12.80° assignable to (110), (200), (210), (220) and (330) Bragg peaks of the same space group. The unit cell parameters obtained from the refined results were well consistent with the predicted values (*Rw*p = 3.07%, *R*p = 2.32% and *Rw*p = 4.47%, *R*p = 3.25% for JUC-635 and JUC-636, respectively). Notably, a similar structure with a 10-fold interpenetrated **dia** net (LZU-79) has been proved by single crystal analysis, and likewise, the PXRD patterns of these COFs were consistent with that from LZU-79 (Figure S5).[21] Therefore,
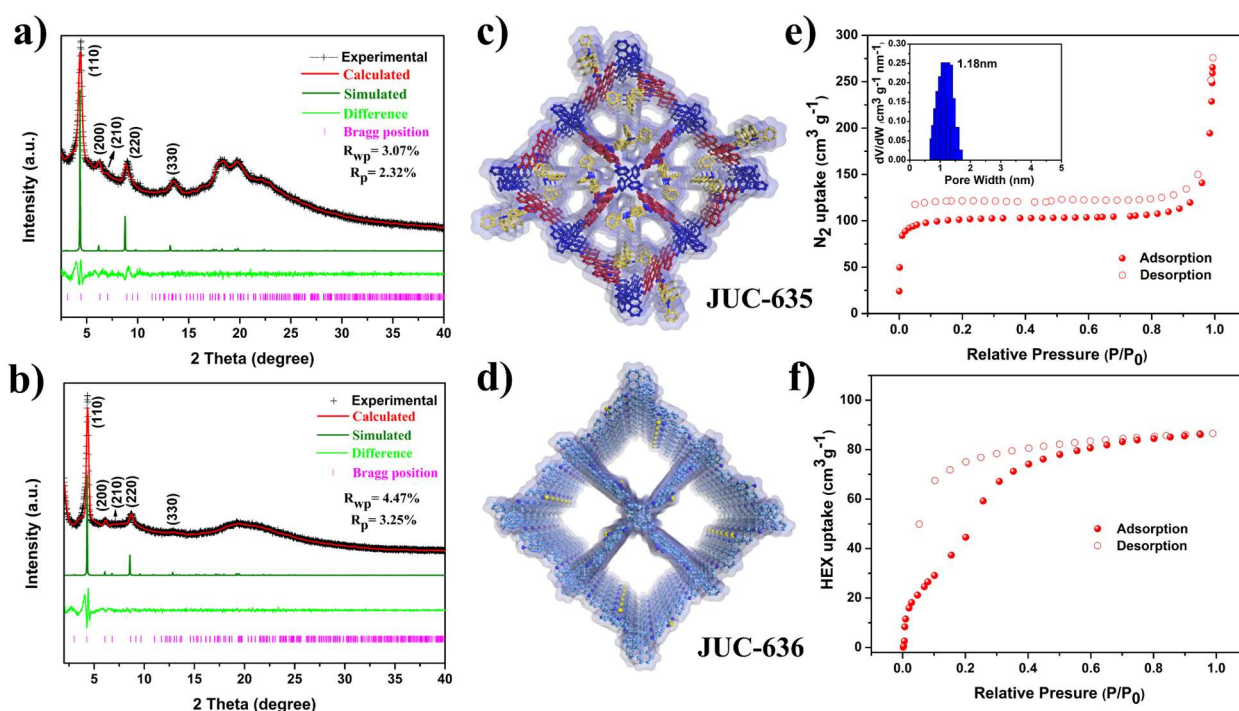
2

Figure 2. PXRD patterns of JUC-635 (a) and JUC-636 (b). Porous structures of JUC-635 (c) and JUC-636 (d) viewed along the *c* axis. N_2 adsorption-desorption isotherm with the pore-size distribution (inset) of JUC-635 (e). Hexane vapor adsorption isotherm of JUC-635 at 298 K, showing dynamic response to vapor pressure (f).

the obtained COFs were considered to have the expected microporous frameworks with 10-fold interpenetrated **dia** topology (Figure 2c,d).

The porosity of these COFs, including specific surface areas and pore sizes, were determined by N_2 adsorption analysis at 77 K (Figures 2e and S6a). A sharp gas uptake could be observed at low pressure of $P/P_0 < 0.05$ for both materials, which revealed their microporous characteristics. The Brunauer–Emmett–Teller (BET) specific surface areas were 398 and 115 m^2 g^{-1} for JUC-635 and JUC-636, respectively (Figure S7). Furthermore, their pore-size distributions calculated by nonlocal density functional theory (NLDFT) demonstrated micropores with diameter sizes of 11.8 and 18.4 Å for JUC-635 and JUC-636, respectively (Figures 2e and S6a, inset), which were in good agreement with pore sizes predicted from their crystal structures (Figure S8a, b). In particular, the molecular TPA units aligned in the same direction between the interpenetrated layers (Figure S8c), and the minimum distance was only 2.5 Å, indicating a strong intermolecular interaction.

In general, 3D imine-linked COFs with **dia** topology are structurally dynamic and undergo geometric changes upon guest release, absorption, and exchange.[18b] This phenomenon is caused by the rotation of the imine bonds, which leads to the backbone contraction. As expected, JUC-635 and JUC-636 also showed similar dynamic behavior (Figures S9 and S10). Taking JUC-635 as an example, the PXRD pattern of the non-activated JUC-635 (soaked in hexane) exhibited identifiable peaks based on its simulated structure but underwent peak disappearance once treated at 60° for 3 hs (Figure S9a,b). Furthermore, when guest-free JUC-635 was re-soaked in hexane at 25 °C for 1 h, its original PXRD pattern recovered (Figure S9c). This process demonstrated the change of symmetry and lattice in JUC-635. We also found that the crystal structure of JUC-635 was sensitive to

the type of included guests. For example, when hexane-loaded JUC-635 was soaked in different solvents, such as *N,N*-dimethylformamide, tetrahydrofuran, dichloromethane, or acetone at 25 °C for 1 h, its original PXRD pattern changed significantly (Figure S9d). However, when solvent-soaked JUC-635 was immersed in hexane again at 25 °C for 1 h, the guest exchange restored its PXRD pattern (Figure S9e). To further verify the breathing effect, hexane-vapor adsorption isotherms were also collected at 298 K (Figures 2f and S6b). Significant stepwise and hysteresis uptakes were observed, indicating that these obtained COFs have dynamic behavior in response to adsorption/desorption processes. These observations allow us to conclude that both materials dynamically change their geometrical feature upon guest release, uptake, and exchange while being able to restore their original structures. This solvent-sensitive response demonstrates the dynamic of frameworks, which thus provides opportunities for these COFs to show pressure-dependent luminescence behavior.

Before applying pressure, we investigated the optical properties of the COFs and their corresponding monomers at atmospheric pressure by UV−Vis absorption and photoluminescence (PL) spectroscopies. As shown in Figure S11, the UV−Vis spectra showed the absorption maximum (λ_{max}) at 416 for JUC-635 and 400 nm for JUC-636, which were slightly shifted compared to those of TPA-BI (425 nm) and BTD (412 nm), giving their yellow color under sunlight. Upon excitation, the emission maximum (λ_{em}) of JUC-635 and its monomer (TPA-BI) appeared 486 and 501 nm, respectively (λ_{ex} = 365 nm). A redder emission was observed in JUC-636 and BTD with λ_{em} at 537 and 510 nm, respectively. The UV-Vis and PL spectra were then measured in different solvents. Remarkably, JUC-635 exhibited solvatochromism, and the wavelength showed a gradual bathochromic shifts ($\Delta\lambda_{em}$ = 72 nm) with increasing solvent
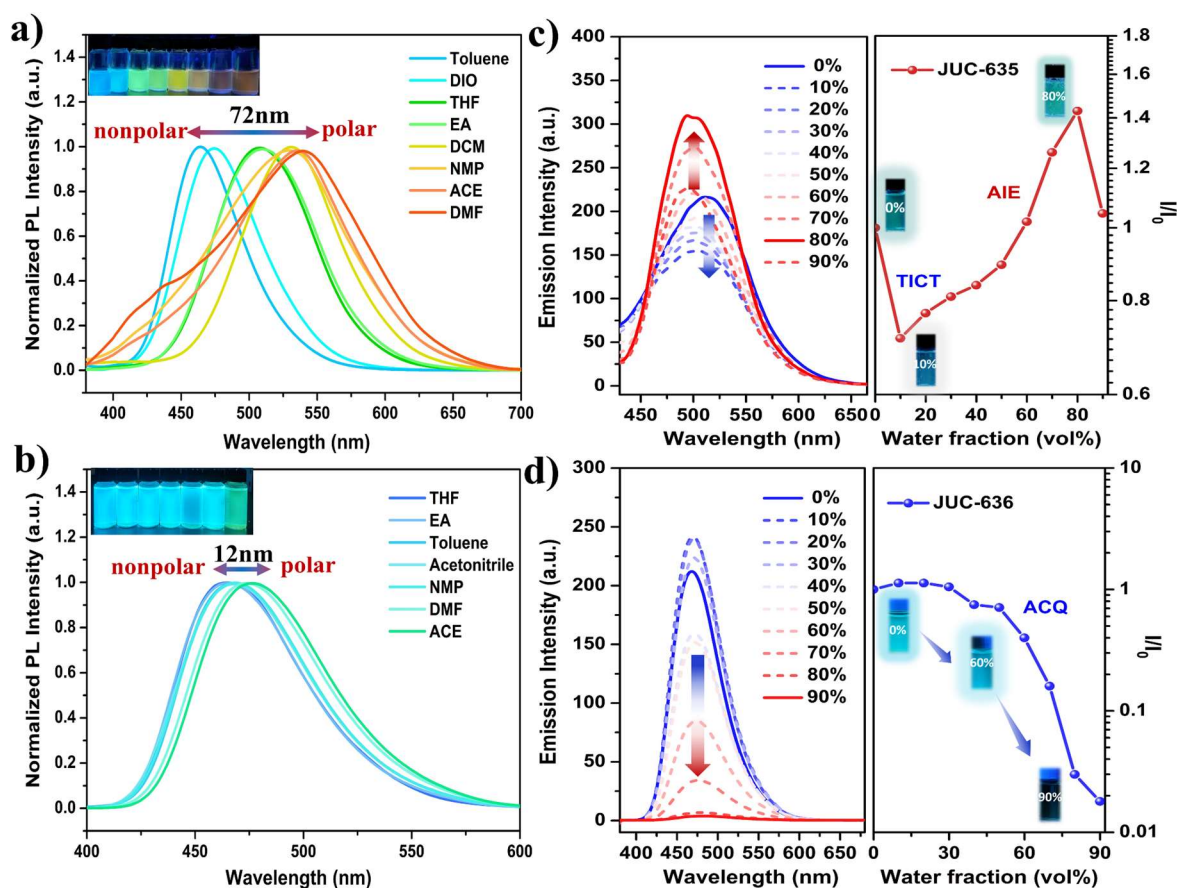
Figure 3. Normalized photoluminescence (PL) spectra and solvatochromism of JUC-635 (a) and JUC-636 (b) in different organic solvents (λ_{ex} = 365 nm). Inset: Photographs of the luminescence. PL spectra in acetonitrile/H$_2$O mixtures with different water fractions (left) and changes in PL peak intensity and emission images in different water fraction mixtures with the excitation wavelength of 365 nm (right) for JUC-635 (c) and JUC-636 (d).

polarity, which could be attributed to the intramolecular charge transfer (ICT) characteristics due to the combination of the electron-donating TPA and the electron-withdrawing BI group (Figures 3a and S12). Moreover, the large bathochromic shifts and broadening of the fluorescence bands in polar solvents, such as *N,N*-dimethylformamide, and *N*-methylpyrrolidone, were observed. These results might arise from the twisted intramolecular charge transfer (TICT) excited state between the TPA and BI units. On the contrary, such unique solvatochromism behaviors have been significantly weakened ($\Delta\lambda_{em}$ = 12 nm) in the case of JUC-636 because of the lack of D-A structure (Figure 3b).

We next sought to understand the aggerate state characteristics of two COFs using mixtures of acetonitrile with water, especially in JUC-635, TPA groups as AIEgens were exposed in the channel rather than locking on the backbone in most reported AIEgen-based COFs.[22] As expected, the TPA-BI monomer exhibited a typical AIE characteristic in acetonitrile /water mixtures (Figure S13). Upon increasing water volume fractions (f_w) from 0% to 30 vol%, the PL intensity of TPA-BI decreased progressively due to the forming of a dark TICT state with an increase in solution polarity. Further amplification of f_w up to 80 vol%, the PL intensity showed a rapid enhancement (AIE effect) because of the suppression of intramolecular rotations decisive to the TICT state through molecular aggregations. More importantly, similar phenomenon can also be observed in JUC-635 (Figure 3c). The PL intensity of JUC-635 decreased with f_w less than 10% because of the TICT effect upon an increase of solution polarity. When f_w was improved from 10 to 90 vol %, the

PL intensity increased significantly and reached the maximum at f_w = 80%. These results suggest a typical TICT+AIE effect of JUC-635, which can be attributed to the enhanced host-guest interactions within the 3D confined space and fine-tuned conformational change of the TPA chromophore.[23] On the contrary, owing to the lack of rotor TPA, JUC-636 exhibited a normal ACQ behavior with gradual fluorescence quenching as the enlargement of water content (Figure 3d), which may show different piezochromism compared with AIEgen-based JUC-635.

Encouraged by the dynamic and photophysical properties of both COFs described above, we investigated their piezochromic behavior by means of isotropic compression based on the DAC technique. As shown in Figure 4a,b, when the pressure was increased from 1 atm to 3 GPa, the PL spectrum of JUC-635 showed nearly maintained fluorescence accompanied by a red-shift from 500 nm to 562 nm. This phenomenon was rather different from most reported cases of piezochromic materials, in which the PL intensity gradually decreased with upgrading the pressure.[24] At the same time, the high sensitivity (20.67 nm GPa^{-1}) of JUC-635 was superior to those observed from two recent reports (18.75 nm GPa^{-1} for NKU-128 and 7.02 nm GPa^{-1} for Sr-ETTB).[19, 24a] Furthermore, JUC-635 exhibited its excellent flexibility by approximately 35 nm shift in emission wavelength within the initial low-pressure range below 1.1 GPa, which was comparable to those of MOFs.[19]

However, once pressure was increased above 3 GPa, the PL intensity of JUC-635 gradually decreased and the emission band continuously red-shifted. When the pressure was up to 12 GPa,
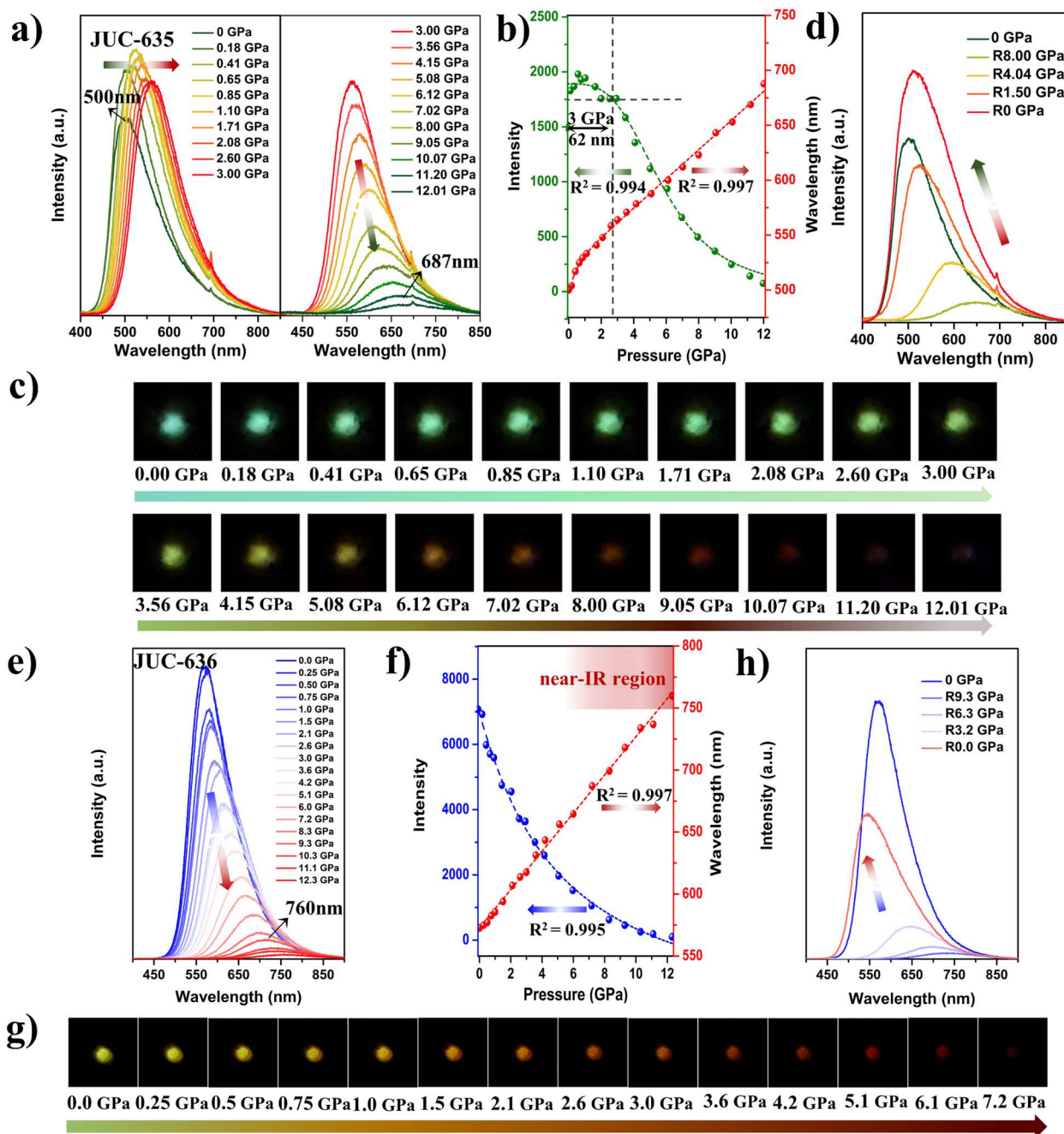
4

Figure 4. Fluorescence spectra and intensity-wavelength plots with corresponding photographs under UV irradiation (λ_{ex} = 355 nm) of JUC-635 (a-c) and JUC-636 (e-g) at various pressures from 1 atm (101 kPa) to 12.01 GPa and 12.3 GPa, respectively. *In-situ* PL spectra of JUC-635 (d) and JUC-636 (h) measured at decreasing pressure upon decompression.

the emission band even shifted to 687 nm and its intensity was relatively featureless. The large wavelength change of 187 nm indicated that high-contrast piezochromism could be achieved in 3D COF by hydrostatic pressure. Notably, this impressive red-shifted emission of JUC-635 ($\Delta\lambda_{em}$ = 187 nm) obtained by isotropic compression (DAC) is higher than most of reported organic small molecule (Figure S14) and much higher than those of piezochromic CPMs obtained by giving anisotropic pressure (grinding or rubbing, Table S1), e.g., 61-fold higher than the lanthanide-viologen ionic MOF (LVMOF-1, $\Delta\lambda_{em}$ = 3 nm),[25] 2-fold higher than tetraphenylethene (TPE) based 3D MOF (Sr-ETTB, $\Delta\lambda_{em}$ = 87 nm) with locking AIEgens on the framework,[24a] and 1.8-fold higher than TPA-based MOF (NKU-128, $\Delta\lambda_{em}$ ≈ 100 nm)

with anchoring AIEgen as side chains onto the skeleton of isolated MOFs.[19] These results indicate that the hydrostatic pressure is a useful tool to explore the piezochromic behavior of COFs, and JUC-635 is suitable for pressure-responsive materials with exotic piezochromic properties.

In-situ fluorescence images of JUC-635 were also taken under pressure from 1 atm to 12.01 GPa, which showed the changes of color from cyan to green and then red with increasing the surrounding pressure (Figure 4c). Not only its ultrawide emitting-color range but also its high sensitivity (15.58 nm GPa^{-1}) is rare, even superior to the record-high value of 14.4 nm GPa^{-1} for 2D perovskite materials.[26] Moreover, in the following decompression process, the emission wavelength and color of
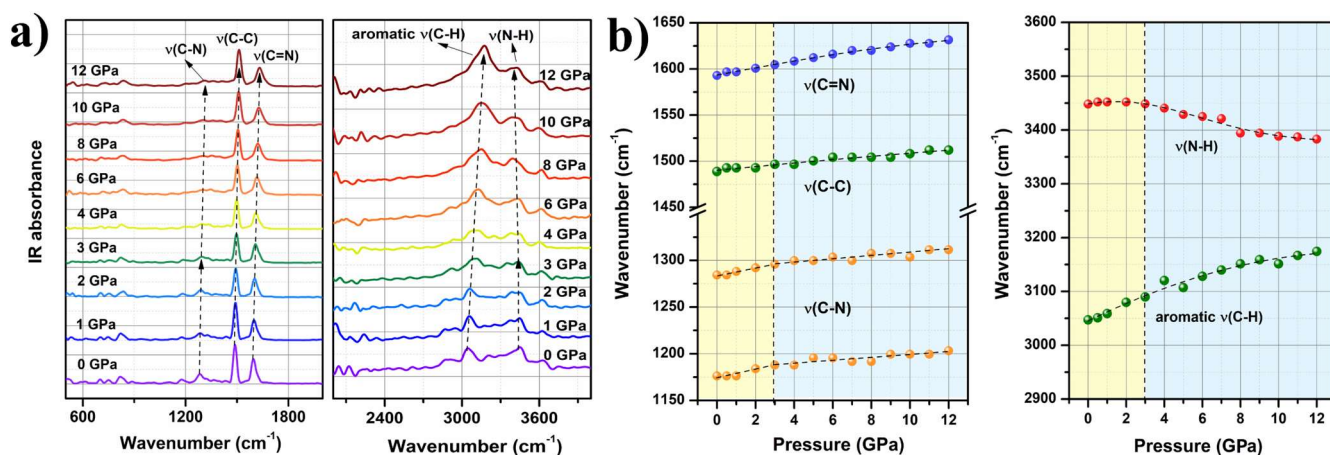
Figure 5. (a) IR spectra of JUC-635 at the range of 0–12 GPa. (b) The pressure dependence of IR peaks of different vibration modes.

JUC-635 could be restored to the original state, and the emission intensity has been slightly increased, suggesting that the pressure-responsive behavior was reversible and the system underwent recovery after gradual decompression as a result of framework relaxation (Figures 4d and S15a).[27] Such a full reversibility phenomenon is unusual since most known piezochromic materials usually exhibit a high-pressure phase residual after pressure release.[28] Therefore, these results confirm that 3D COFs have a great potential for the development of high-contrast piezochromic materials with remarkable emission differences, high sensitivity, and excellent reversibility.

As a comparison, the solid-state fluorescence of JUC-636 at different pressures was investigated. Different from JUC-635, the emission intensity of JUC-636 suffered a rapid decline with 51% when increasing pressure to 3 GPa, and its fluorescence was basically quenched at 12.3 GPa with a wavelength change of 183 nm (Figure 4e,f). *In-situ* fluorescence images showed the PL color of JUC-636 became dark red, and the PL brightness gradually decreased. No obvious red color was observed after 7.2 GPa owing to the spanning of the deep red (687 nm) to the near-infrared region (760 nm, Figures 4g and S15b), but weak fluorescence could be detected until 12.3 GPa. When the pressure was released to 0 GPa upon decompression, the emission wavelength was restored to the original state, but the emission intensity suffered a certain decline owing to the slower framework relaxation speed of empty pores (Figures 4h and S15c). Obviously, the twisted TPA unit of JUC-635 plays an important role in the maintained fluorescence before 3 GPa as well as the full reversibility under pressure. We presume that the hydrostatic pressure can effectively inhibit the free movement of propeller-like AIEgen to maintain the fluorescence without quenching, and the presence of TPA in the pores facilitates the recovery of the framework. The monomer TPA-BI showed a similar pressure response effect compared to JUC-635 (Figure S16), but the emission intensity could be only stable at 0-1.6 GPa. This indicates that the relative rigidification of framework resists the pressure through deformation and further limits the rotation of TPA as a "secondary stimulus" with the increased pressure.

To explore the working mechanism of piezochromism at a molecular level, a set of high-pressure *in-situ* FT-IR spectra of JUC-635 was recorded in DAC. As shown in Figure 5a, the bands at 1284 and 1488 cm^{-1} were assigned as the stretching vibration of C-N (v(C–N)) and C-C (v(C–C)), respectively. Meanwhile, the

band at 1609 cm^{-1} was the stretching vibration of C=N (v(C=N)), characteristic of the imine bond, while at 3047 and 3448 cm^{-1} were the stretching vibration of aromatic C-H (v(C–H)) and N-H (v(N-H)), respectively. After applying pressure from 0 to 12 GPa, the vibration bands of the most functional groups shifted to the higher wavenumber (Figure 5b), revealing that the pressure activated those functional groups of JUC-635 by strengthening the bonds and increasing their vibration frequency. Especially, the characteristic peak of the imine bond (v(C=N)) was much more blue-shifted than other functional groups, indicating that imine bonds were more susceptible to pressure. Meanwhile, the vibration bands of v(C-N) shifted to a higher wavenumber, accompanied by a shift rate of 3.86 cm^{-1}/GPa at 0–3 GPa and 1.71 cm^{-1}/GPa at 3–12 GPa. Such a similar tendency could also be observed in the aromatic C-H (v(C–H)) (14 cm^{-1}/GPa at 0–3 GPa and 9.4 cm^{-1}/GPa at 3–12 GPa), indicating that the twisted TPA in the empty pores was largely affected before 3 GPa and restricted after 3 GPa. Moreover, we noticed that v(N-H) peak of imidazole shifted to higher wavenumber at the beginning but had an obvious redshift after 3 GPa, which could be attributed to the strengthened N–H…N hydrogen bonds because of the reduced distance between the imidazole rings. Before compression, the distance between adjacent penetrated layers of JUC-635 was 7.55 Å, which was not suitable for the formation of hydrogen bonds, but the generation of N–H…N after compression indicated that the distance between penetrated layers was significantly shortened due to the van der Waals forces.

Overall, in the compression process of 0–3 GPa, the stretching vibration of the imine bond lead to the deformation of the framework, which further enhanced the interaction between the TPA molecules in the pores and largely limited the TPA molecules. Due to the restriction of freely rotating benzene rings of TPA, the non-radiative decay reduced and did not significantly change the fluorescence before 3 GPa. It should be noted that NKU-128, a similar structure to JUC-635, behaved similarly,[19] i.e., the space deformation induced by outer stimuli acts as a "secondary stimulus" to trigger and regulate the conformational changes of the organic chromophore structure. At higher pressure (> 3 GPa), the shorter distance between penetrated layers increased the possibility of hydrogen bonds, but the vibration of other bonds was further strengthened, resulting in the increase of the non-radiative process as a leading role in fluorescence quenching after 3 GPa. In this case, the synergy between the

twisted conformation and dynamic penetrated framework determines the excellent piezochromic behavior of JUC-635.

In summary, we have designed and synthesized two new 3D COFs (JUC-635 and JUC-636) with 10-fold interpenetrated **dia** nets and structural breathing flexibility. By rationally regulating the structures, these COFs had distinct solvatochromism and molecular aggregation behavior in solvents. Based on their dynamic framework and fluorescence properties, for the first time, we explored the piezochromism of COFs at high pressure by DAC experiment. JUC-635 maintained its fluorescence before 3 GPa and exhibited a reversible piezochromism upon 12 GPa, which was rather different from the continuous fluorescence reduction shown by JUC-636. Remarkably, high contrast piezochromism with significant emission differences ($\Delta\lambda_{em}$ = 187 nm) were achieved by JUC-635, which was the highest among CPMs reported so far. These results thus confirm that 3D COFs have a great potential for the development of piezochromic materials with outstanding emission differences, high sensitivity, and excellent reversibility. More relevant works will be carried out in this field, including pressure-induced emission enhancement, the relationship between structural changes and fluorescence, and the interaction of host-guest under pressure.

Acknowledgements

[1] a) N. Huang, X. Ding, J. Kim, H. Ihee, D. Jiang, *Angew. Chem. Int. Ed.* **2015**, *54*, 8704-8707; b) L. Wang, K.-Q. Ye, H.-Y. Zhang, *Chin Chem Lett.* **2016**, *27*, 1367-1375; c) A. Deak, C. Jobbagy, G. Marsi, M. Molnar, Z. Szakacs, P. Baranyai, *Chem. Eur. J.* **2015**, *21*, 11495-11508; d) X. Zhao, P. Alam, J. Zhang, S. Lin, Q. Peng, J. Zhang, G. Liang, S. Chen, J. Zhang, H. H. Y. Sung, J. W. Y. Lam, I. D. Williams, X. Gu, Z. Zhao, B. Z. Tang, *CCS Chem.* **2022**, *4*, 2570-2580.

[2] a) C. R. Martin, G. A. Leith, P. Kittikhunnatham, K. C. Park, O. A. Ejegbavwo, A. Mathur, C. R. Callahan, S. L. Desmond, M. R. Keener, F. Ahmed, S. Pandey, M. D. Smith, S. R. Phillpot, A. B. Greytak, N. B. Shustova, *Angew. Chem. Int. Ed.* **2021**, *60*, 8072-8080; b) G. A. Leith, C. R. Martin, J. M. Mayers, P. Kittikhunnatham, R. W. Larsen, N. B. Shustova, *Chem. Soc. Rev.* **2021**, *50*, 4382-4410.

[3] a) Z.-Z. Lu, R. Zhang, Y.-Z. Li, Z.-J. Guo, H.-G. Zheng, *J. Am. Chem. Soc.* **2011**, *133*, 4172-4174; b) G. Mehlana, S. A. Bourne, *CrystEngComm.* **2017**, *19*, 4238-4259.

[4] Z. H. Zhu, C. Bi, H. H. Zou, G. Feng, S. Xu, B. Z. Tang, *Adv. Sci.* **2022**, *9*, e2200850.

[5] a) A. Sussardi, C. L. Hobday, R. J. Marshall, R. S. Forgan, A. C. Jones, S. A. Moggach, *Angew. Chem. Int. Ed.* **2020**, *59*, 8118-8122; b) C. X. Chen, S. Y. Yin, Z. W. Wei, Q. F. Qiu, N. X. Zhu, Y. N. Fan, M. Pan, C. Y. Su, *Angew. Chem. Int. Ed.* **2019**, *58*, 14379-14385.

[6] C.-X. Chen, Z.-W. Wei, C.-C. Cao, S.-Y. Yin, Q.-F. Qiu, N.-X. Zhu, Y.-Y. Xiong, J.-J. Jiang, M. Pan, C.-Y. Su, *Chem. Mater.* **2019**, *31*, 5550-5557.

[7] a) Z. Chi, X. Zhang, B. Xu, X. Zhou, C. Ma, Y. Zhang, S. Liu, J. Xu, *Chem. Soc. Rev.* **2012**, *41*, 3878-3896; b) K. Maity, D. Mukherjee, M. Sen, K. Biradha, *ACS Appl. Nano Mater.* **2019**, *2*, 1614-1620; c) ; d) M. Li, G. Ren, W. Yang, Y. Yang, W. Yang, Y. Gao, P. Qiu, Q. Pan, *ChemComm.* **2021**, *57*, 1340-1343; e) W. Wang, R. Li, S. Xiao, Q. Xing, X. Yan, J. Zhang, X. Zhang, H. Lan, T. Yi, *CCS Chem.* **2022**, *4*, 899-909; f) Z. Ma, F. Li, D. Zhao, G. Xiao, B. Zou, *CCS Chem.* **2020**, *2*, 71-80.

[8] a) Q. Zhang, J. Su, D. Feng, Z. Wei, X. Zou, H. C. Zhou, *J. Am. Chem. Soc.* **2015**, *137*, 10064-10067; b) M. Andrzejewski, A. Katrusiak, *J. Phys. Chem. Lett.* **2017**, *8*, 279-284; c) Z. Q. Yao, J. Xu, B. Zou, Z. Hu, K. Wang, Y. J. Yuan, Y. P. Chen, R. Feng, J. B. Xiong, J. Hao, X. H. Bu, *Angew. Chem. Int. Ed.* **2019**, *58*, 5614-5618; d) A. Li, S. Xu, C. Bi, Y. Geng, H. Cui, W. Xu, *Mater. Chem. Front.* **2021**, *5*, 2588-2606.

[9] a) A. P. Cote, A. I. Benin, N. W. Ockwig, M. O'Keeffe, A. J. Matzger, O. M. Yaghi, *Science.* **2005**, *310*, 1166-1170; b) H. M. El-Kaderi, J. R. Hunt, J. L. Mendoza-Cortes, A. P. Cote, R. E. Taylor, M. O'Keeffe, O. M. Yaghi, *Science.* **2007**, *316*, 268-272; c) X. Feng, X. Ding, D. Jiang, *Chem. Soc. Rev.* **2012**, *41*, 6010-6022; d) M. S. Lohse, T. Bein, *Adv. Funct. Mater.* **2018**, *28*, 1705553; e) X. Guan, F. Chen, Q. Fang, S. Qiu, *Chem. Soc. Rev.* **2020**, *49*, 1357-1384; f) X. Guan, Q. Fang, Y. Yan, S. Qiu, *Acc. Chem. Res.* **2022**, *55*, 1912-1927.

[10] a) S. Kim, H. C. Choi, *Commun. Chem.* **2019**, *2*, 60; b) Y. Liu, J. Ren, Y. Wang, X. Zhu, X. Guan, Z. Wang, Y. Zhou, L. Zhu, S. Qiu, S. Xiao, Q. Fang, *CCS Chem.* **2023**, doi.org/10.31635/ccschem.022.202202352.

[11] a) X. Liu, J. Li, B. Gui, G. Lin, Q. Fu, S. Yin, X. Liu, J. Sun, C. Wang, *J. Am. Chem. Soc.* **2021**, *143*, 2123-2129; b) M. Zhang, J. Fang, Y. Liu, Y. Wang, L. Liao, L. Tang, L. Zhu, S. Qiu, Q. Fang, *Small Structures.* **2021**, *2*, 2000108.

[12] W. Zhao, C. Yu, J. Zhao, F. Chen, X. Guan, H. Li, B. Tang, G. Yu, V. Valtchev, Y. Yan, S. Qiu, Q. Fang, *Small.* **2021**, *17*, 2102630.

[13] A. M. Kaczmarek, Y. Y. Liu, M. K. Kaczmarek, H. Liu, F. Artizzu, L. D. Carlos, P. Van Der Voort, *Angew. Chem. Int. Ed.* **2020**, *59*, 1932-1940.

[14] a) W. K. Haug, E. M. Moscarello, E. R. Wolfson, P. L. McGrier, *Chem. Soc. Rev.* **2020**, *49*, 839-864; b) P. She, Y. Qin, X. Wang, Q. Zhang, *Adv. Mater.* **2022**, *34*, e2101175; c) Y. Liu, X. Guan, Q. Fang, *Aggregate.* **2021**, *2*, e34.

[15] a) Z. Fu, K. Wang, B. Zou, *Chin Chem Lett.* **2019**, *30*, 1883-1894; b) T. Gong, Q. Sui, P. Li, X. F. Meng, L. J. Zhou, J. Chen, J. Xu, L. Wang, E. Q. Gao, *Small.* **2019**, *15*, e1803468; c) H. Liu, Y. Gu, Y. Dai, K. Wang, S. Zhang, G. Chen, B. Zou, B. Yang, *J. Am. Chem. Soc.* **2020**, *142*, 1153-1158; d) A. Sussardi, C. L. Hobday, R. J. Marshall, R. S. Forgan, A. C. Jones, S. A. Moggach, *Angew. Chem.* **2020**, *132*, 8195-8199; e) X. Wang, C. Qi, Z. Fu, H. Zhang, J. Wang, H. T. Feng, K. Wang, B. Zou, J. W. Y. Lam, B. Z. Tang, *Mater. Horiz.* **2021**, *8*, 630-638.

[16] J. Sun, A. Iakunkov, I. A. Baburin, B. Joseph, V. Palermo, A. V. Talyzin, *Angew. Chem. Int. Ed.* **2020**, *59*, 1087-1092.

[17] W. Liu, Y. Cao, W. Wang, D. Gong, T. Cao, J. Qian, K. Iqbal, W. Qin, H. Guo, *ChemComm.* **2018**, *55*, 167-170.

[18] a) T. Sun, L. Wei, Y. Chen, Y. Ma, Y. B. Zhang, *J. Am. Chem. Soc.* **2019**, *141*, 10962-10966; b) Y. X. Ma, Z. J. Li, L. Wei, S. Y. Ding, Y. B. Zhang, W. Wang, *J. Am. Chem. Soc.* **2017**, *139*, 4995-4998; c) Y. Chen, Z.-L. Shi, L. Wei, B. Zhou, J. Tan, H.-L. Zhou, Y.-B. Zhang, *J. Am. Chem. Soc.* **2019**, *141*, 3298-3303.

[19] Z. Q. Yao, K. Wang, R. Liu, Y. J. Yuan, J. J. Pang, Q. W. Li, T. Y. Shao, Z. G. Li, R. Feng, B. Zou, W. Li, J. Xu, X. H. Bu, *Angew. Chem. Int. Ed.* **2022**, *61*, e202202073.

[20] a) Q. Qi, J. Qian, X. Tan, J. Zhang, L. Wang, B. Xu, B. Zou, W. Tian, *Adv. Funct. Mater.* **2015**, *25*, 4005-4010; b) Y. Zhang, M. Qile, J. Sun, M. Xu, K. Wang, F. Cao, W. Li, Q. Song, B. Zou, C. Zhang, *J. Mater. Chem. C.* **2016**, *4*, 9954-9960; c) Y. Zhang, K. Wang, G. Zhuang, Z. Xie, C. Zhang, F. Cao, G. Pan, H. Chen, B. Zou, Y. Ma, *Chem. Eur. J.* **2015**, *21*, 2474-2479.

[21] T. Ma, E. A. Kapustin, S. X. Yin, L. Liang, Z. Zhou, J. Niu, L. H. Li, Y. Wang, J. Su, J. Li, X. Wang, W. D. Wang, W. Wang, J. Sun, O. M. Yaghi, *Science.* **2018**, *361*, 48-52.

[22] J. Dong, X. Li, S. B. Peh, Y. D. Yuan, Y. Wang, D. Ji, S. Peng, G. Liu, S. Ying, D. Yuan, J. Jiang, S. Ramakrishna, D. Zhao, *Chem. Mater.* **2018**, *31*, 146-160.

[23] S. Liu, Y. Li, R. T. Kwok, J. W. Lam, B. Z. Tang, *Chem. Sci.* **2021**, *12*, 3427-3436.

[24] a) X. Guo, N. Zhu, S. P. Wang, G. Li, F. Q. Bai, Y. Li, Y. Han, B. Zou, X. B. Chen, Z. Shi, S. Feng, *Angew. Chem. Int. Ed.* **2020**, *59*, 19716-19721; b) X. Wang, C. Qi, Z. Fu, H. Zhang, J. Wang, H.-T. Feng, K. Wang, B. Zou, J. W. Lam, B. Z. Tang, *Mater. Horizons.* **2021**, *8*, 630-638.

[25] T. Gong, Q. Sui, P. Li, X.-F. Meng, L.-J. Zhou, J. Chen, J. Xu, L. Wang, E.-Q. Gao, *Small.* **2019**, *15*, 1803468.

[26] Y. Fang, L. Zhang, Y. Yu, X. Yang, K. Wang, B. Zou, *CCS Chem.* **2021**, *3*, 2203-2210.

[27]   Z. Q. Yao, J. Xu, B. Zou, Z. Hu, K. Wang, Y. J. Yuan, Y. P. Chen, R. Feng, J. B. Xiong, J. Hao, X. H. Bu, *Angew. Chem.* **2019**, *131*, 5670-5674.

[28]   a) L. Wang, K. Wang, B. Zou, K. Ye, H. Zhang, Y. Wang, *Adv. Mater.* **2015**, *27*, 2918-2922; b) Y. Wang, X. Tan, Y. M. Zhang, S. Zhu, I. Zhang, B. Yu, K. Wang, B. Yang, M. Li, B. Zou, S. X. Zhang, *J. Am. Chem. Soc.* **2015**, *137*, 931-939.

8

Entry for the Table of Contents
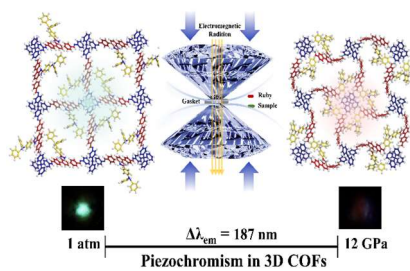
Dynamic three-dimensional covalent organic frameworks based on aggregation-induced emission or aggregation-caused quenching chromophores have been successfully prepared, and for the first time were used to study the piezochromism under mechanical stimuli by diamond anvil cell technique.